Optimization of High-Speed White Beam X-ray Imaging for Spray Characterization

Timothy B. Morgan*, Julie K. Bothell, Thomas J. Burtnett,
Danyu Li, and Theodore J. Heindel
Center for Multiphase Flow Research and Education
Department of Mechanical Engineering
Iowa State University
Ames, IA 50011 USA

Alberto Aliseda and Nathanael Machicoane
Department of Mechanical Engineering
University of Washington
Seattle, WA 98195 USA

Katarzyna Matusik and Alan L. Kastengren
X-ray Science Division, Advanced Photon Source
Argonne National Laboratory
Argonne, IL 60439 USA

Abstract

The near-field region of a spray has a significant impact on the downstream dynamics. However, the near-field region remains one of the most difficult areas to characterize due to its optical density to visible light. One of the methods used to probe the near-field region is high-speed white beam (broad-spectrum) X-ray radiography, which generates path integrated, time sequenced images of the spray. While white beam imaging is effective at probing the near-field region, high intensity synchrotron sources are required to acquire high-speed time-resolved image sequences. The drawback to a synchrotron source is it emits a significant portion of its X-ray spectrum at energies that are minimally attenuated by most sprays. This paper will examine the various parameters that can be tuned to improve the characterization of sprays with white beam X-rays, and will assess their effects on the X-ray image quality. A representative spray conditions will be shown using a canonical coaxial gas-liquid atomizer imaged at the 7-BM beamline of the Advanced Photon Source at Argonne National Laboratory.

* Corresponding author, tbmorgan@iastate.edu

Introduction

X-ray radiography has been used to image a wide range of multiphase flows, from very dense flows, such as fluidized beds, to very dispersed flows, such as sprays [1–4]. X-ray radiography is particularly useful with multiphase flows due to the ability of X-rays to penetrate through optically opaque materials with minimal scattering and refraction. However, in dispersed flows there is often minimal material to attenuate the X-rays, which can result in a weak signal. Specifically, when X-ray imaging sprays, the liquid core has a small cross section (2.1 mm in this study), and the diameter of individual droplets can be two or more orders of magnitude smaller. Additionally, the most commonly used fluids in the study of sprays are air and water. Air is almost completely X-ray transparent, and water is only strongly absorbing at lower photon energies (soft X-rays). Finally, the high velocities that occur in sprays require high X-ray powers to provide sufficient flux to the detector to use short exposure times while still maintaining a good signal-to-noise ratio.

Multiple approaches have been used to provide the best possible X-ray radiography data. One approach is focused beam radiography [5, 6]. In focused beam radiography, a powerful X-ray source (typically a synchrotron source) is passed through a monochromator to filter the beam to a narrow range of photon energies. After it has been filtered, the beam is focused (using X-ray mirrors at a very shallow grazing angle) to make the spot size as small as possible. This method is advantageous because the beam flux is relatively high, allowing for very fast measurements. The use of monochromatic X-rays also allows for the direct computation of the pathlength of material through which the X-rays pass. The downside of focused beam imaging is that the X-ray spot size is so small (on the order of a few microns) that only a very small portion of the spray can be measured at once. Therefore, focused beam radiography is typically used as a point measurement and raster scanning across the spray is required to quantify the full spray.

Another approach to optimizing X-ray imaging of sprays is monochromatic beam imaging [7]. Monochromatic beam imaging is similar to focused beam in that a powerful X-ray beam is filtered to a narrow range of energies by a monochromator. However, unlike focused beam imaging, the filtered beam is left as large as possible allowing for a relatively large region (on the order of a few mm wide) to be imaged. Like focused beam imaging, monochromatic beam imaging allows for the direct computation of the pathlengh of material through which the X-rays pass. However, because the beam is not focused, the intensity of the X-ray beam is relatively low, resulting in a low signal-to-noise ratio and limited ability to capture high speed spray features.

For imaging a large area at high speed, the best option is white beam radiography [8, 9]. Unlike focused beam and monochromatic beam radiography, in white beam radiography both the full size and full energy spectrum of the X-ray source are used. With a powerful X-ray source, e.g. a synchrotron source, there is sufficient beam power to do imaging at high speed, with extremely short exposures, which minimizes motion blur. One of the drawbacks of white beam imaging is that a large portion of the white beam X-ray spectrum is at energy levels that are minimally attenuating by fluids of interest for sprays. There are two approaches to solve this: (i) the beam spectrum can be modified with filters so that a large percentage of the remaining photons are at energies that are attenuated by the fluid, or (ii) a contrast material can be added to the fluid to provide greater attenuation at the energies that are more prominent in the white beam spectrum [10, 11].

This work examines the effects of both X-ray filters and X-ray contrast material on the resulting radiographs. This is first done by simulating the X-ray spectrum with various X-ray filters in the beam and the absorption of different contrast materials. For comparison to the simulated data, a real spray is tested with various X-ray filters and with different contrast materials added to the liquid. Additionally, two different scintillator materials are tested as X-ray detectors.

Experimental Setup

All of the experiments in this study were performed at the 7-BM beamline of the Advanced Photon Source at Argonne National Laboratory. The 7-BM beamline is dedicated to the time-resolved study of highly dynamic fluid flows, particularly sprays [6]. It uses a 0.599 T bending magnet to produce X-rays by bending the path of the 7 GeV electrons in the storage ring. As shown in Figure 1, when doing white beam imaging, the X-ray beam is first filtered by an optional filter to change the X-ray spectrum, and then passes through a chopper wheel. The chopper wheel briefly blocks the X-ray beam to reduce the average power on the detector and minimize the chances of thermal damage. After the chopper wheel, the beam passes through the object of interest (in this case a spray) and onto a scintillator, which converts the X-ray photons into visible light photons. Two different scintillators are used in this study, a yttrium-aluminum garnet (YAG) scintillator and a lutetium-aluminum garnet (LuAG) scintillator. Finally, the scintillator is imaged

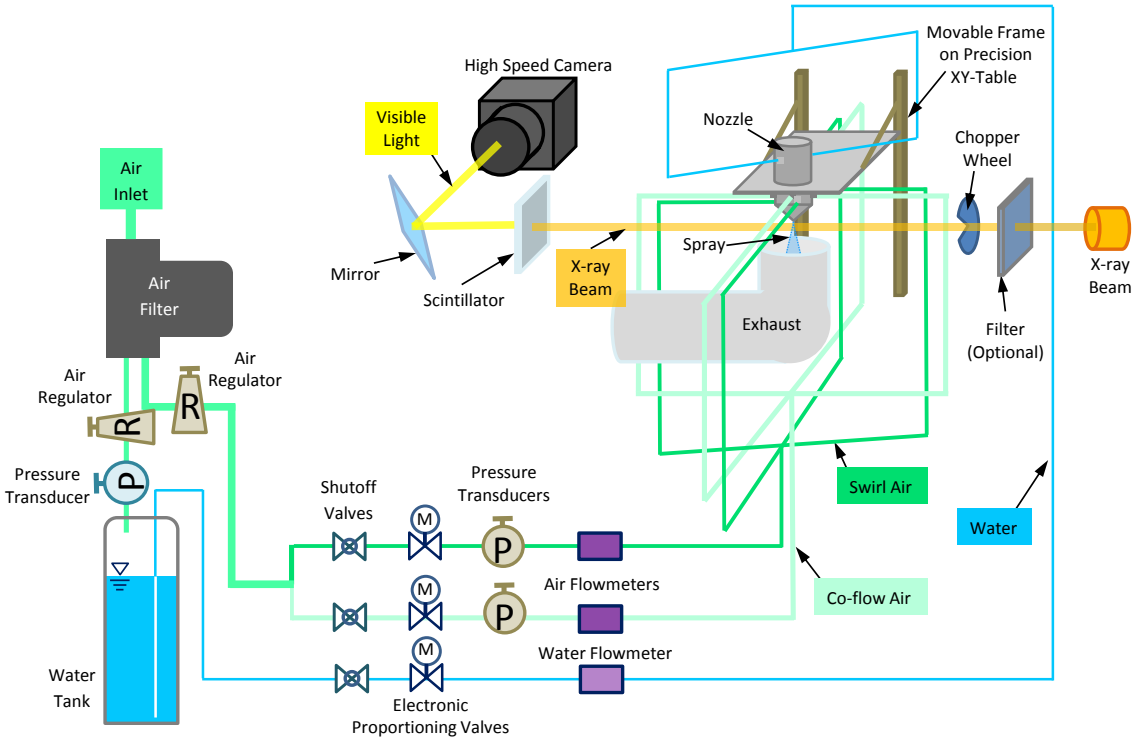

Figure 1. A schematic of the co-axial flow gas-liquid spray nozzle setup for white beam imaging at the 7-BM beamline of the Advanced Photon Source.

with a turning mirror and macro-coupled lens pair on a high speed camera (a Photron SA-Z in this study). The use of the mirror is necessary to minimize radiation exposure on the optics and electronics of the camera.

The spray used in this study is from a gas-liquid coaxial atomizer. Liquid (water with optional contrast material in this study) is injected through an inner nozzle with an inner diameter of d_l = 2.1 mm and an outer diameter of D_l = 2.7 mm. Surrounding the inner nozzle is an outer nozzle through which gas (compressed air) is injected. The outer nozzle has an inner diameter d_g = 10 mm. The gas can be injected into the outer nozzle both perpendicular to the liquid nozzle and tangentially to the outer nozzle wall to produce either a straight co-flow of air, a swirling airflow, or a mixture of both. All spray tests in this paper were at a liquid flow rate of Q_l = 0.099 LPM and a co-flow gas flow rate of Q_{NS} = 150 LPM. No swirling gas flow was used in this study. More information about the spray nozzle can be found in [12].

To optimize the imaging parameters for white beam imaging, three different parameters were varied. First, the spray was tested with four different filtering configurations – unfiltered, a 500 µm thick silicon filter, a 50 µm thick copper filter, and a 25 µm thick molybdenum filter. The effect of these filters was also simulated in the XOP X-ray simulation software to determine the effect on the spectrum of the X-ray beam [13]. Second, the spray was tested without any contrast material in the water, with 7.0% by mass KI, and with 5.0% by mass KI and 0.5% by mass NaBr. The effect on the X-ray mass attenuation coefficient was determined using the XCOM X-ray cross sections database and compared with experimental results [14]. Finally, two different scintillators (a 500 µm thick YAG and 100 µm thick LuAG) were tested to determine the effect of the scintillator on the resulting image.

Results

Before comparing the effects of the various parameters, it is first important to understand the unfiltered X-ray spectrum of the 7-BM beamline. The spectrum, as simulated by XOP, is shown in Figure 2. It is important to note that the spectrum is extremely broad, stretching from <1 keV all the way to 7 GeV. However, it should also be noted that the majority of the power of the spectrum occurs at <100keV. Additionally, the raw beam is filtered before entering the experiment hutch by a 500 µm thick beryllium window that terminates the vacuum section of the beam pipe, which removes most of the spectrum below 2 keV. Therefore, the remainder of the spectrum plots will only show the range from 1 keV to 100 keV, with the understanding that a small portion of the X-ray power does occur outside the plotted range.

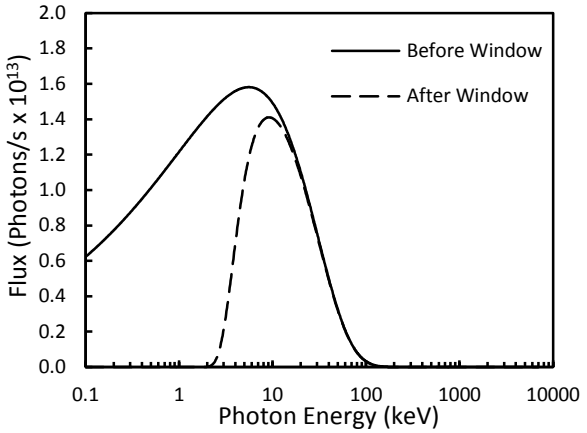

Figure 2. The X-ray spectrum of the white beam at the 7-BM beamline before and after filtering by the 500 μm thick beryllium window.

Effect of X-ray Filters

To examine the effects of filtering on spray imaging, the simulated spectrum of various filters was calculated in XOP for the range where most of the flux occurs (1 keV to 100 keV). Figure 3 shows these spectrums for the X-ray beam before the beryllium window, filtered by only the beryllium window, filtered by the beryllium window and a 500 μm thick silicon filter, filtered by the beryllium window and a 50 μm thick copper filter, and filtered by the beryllium window and a 25 μm thick molybdenum filter. It should be noted, that the beam spectrum before the beryllium window is only for reference purposes. This beam can only occur within the vacuum of the beam pipe; therefore, it is not possible to use it for imaging. Due to this, the beam as filtered by the 500 μm thick beryllium window will be referred to as the "unfiltered" beam going forward.

From Figure 3, it is clear that all filtering causes a significant reduction in X-ray flux, particularly at low photon energies where water is the most attenuating (see Figure 6 for reference). The reduction in total means that applying any filtering will lower the X-ray flux, which in turn produces a lower visible light output from the scintillator, and requires longer exposure times to achieve the same recorded intensity on the camera, which in turn could introduce more motion blur. Specifically, by integrating the X-ray spectrum in XOP, it was determined that the 500 μm silicon filtered beam should produce an intensity of 68% that of the unfiltered beam. The 50 μm copper filter should produce a beam with 53% of the intensity of the unfiltered beam, and the 25 μm molybdenum filter should produce a beam with 55% of the intensity of the unfiltered beam. Additionally, the reduction in flux at

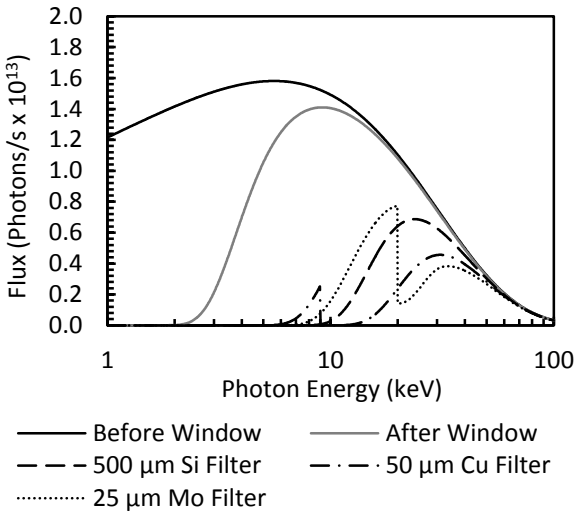

Figure 3. The simulated X-ray spectrums for the 7-BM beamline before the beryllium window, after the beryllium window, and after the beryllium window with various filters applied.

the low energies will result in decreased contrast on the image for the same recorded intensity on the camera.

Figure 4 shows the effect of the filtering on a real spray, imaged at the exit of the spray nozzle. It is immediately clear that the molybdenum filter causes a significant reduction in intensity. The measured beam intensity with the molybdenum filter is 16% of the measured unfiltered beam intensity, both measured as the average intensity in a 9000 pixel region containing no liquid. The copper and silicon filters also cause a drop in intensity, although not as significant as the molybdenum filter. The 50 μm copper filtered beam has a measured intensity of 47% of the unfiltered beam and the 500 μm silicon filtered beam has a measured intensity of 71% of the unfiltered beam. The copper and silicon filter both produce reductions in intensity that are in line with what XOP predicts. However, there is a significant difference between the predicted intensity and the measured intensity for the molybdenum filtered beam. This is believed to be because the filtered beam measurements were done using the 500 μm thick YAG scintillator, which has a reduction in conversion efficiency from 12 keV to 17 keV. This reduction in efficiency closely matches the peak flux of the 25 μm molybdenum filtered beam. Therefore, it is speculated that the molybdenum filter may be more useful if a different scintillator material is used.

In addition to the intensity changes, the silicon filter also appears to reduce the visibility of the background pattern (which are small scratches on the beryllium window). However, the same result can be

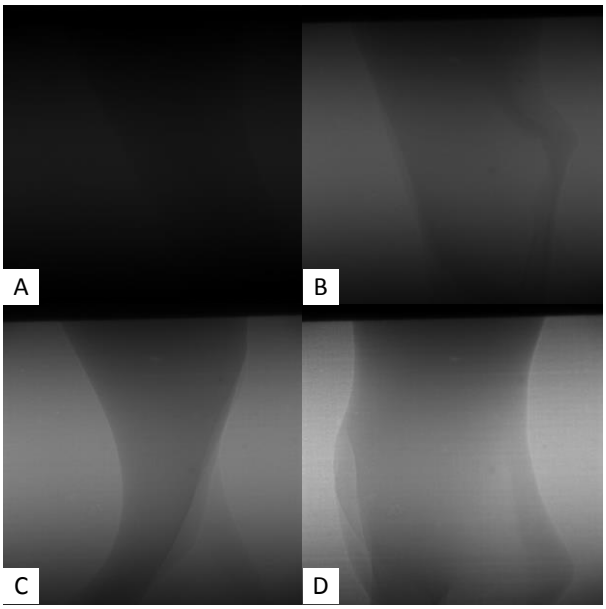

Figure 4. The exit of the spray nozzle imaged with four different X-ray filters A) 25 μm thick molybdenum, B) 50 μm thick copper, C) 500 μm thick silicon, and D) unfiltered. All images were taken with an exposure of 2.5 microseconds.

achieved using flat field correction [15], which has not been applied here for the sake of demonstrating the effects of filtering on the raw images. Finally, it should be noted that all the images in Figure 4 were acquired with the same exposure time (2.5 μs). The intensity difference could be resolved by increasing the exposure time for the filtered images, but would risk introducing motion blur in the images, particularly at higher flow rates.

Finally, it should be noted that while running with the unfiltered X-ray beam has advantages for the resulting image, the power of the beam also produces some challenges. First, the power of the beam can cause the scintillator to heat up, which slightly changes its light output. If the scintillator is exposed to the beam for too long, without being allowed to cool, irreversible thermal damage can occur. Second, the cumulative effects of radiation exposure can cause damage to the instrumentation and experiment. Figure 5 shows radiation damage on the acetal plastic outer wall of the spray nozzle due to exposure to the X-ray beam.

Effect of Contrast Material

The second method of improving the contrast of the spray for X-ray imaging is to add a contrast material to the liquid. Contrast agents can be any material that is soluble in the liquid, with a high X-ray attenuation (which in practice means a high atomic number).

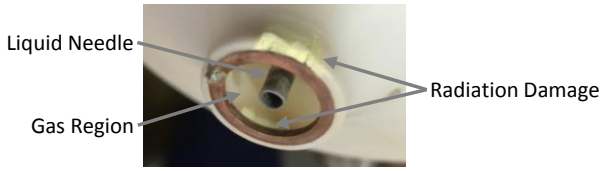

Figure 5. Radiation damage on the spray nozzle due to extended exposure to high-intensity radiation. Note that the damage occurs throughout the path of the X-rays, not just on the surface.

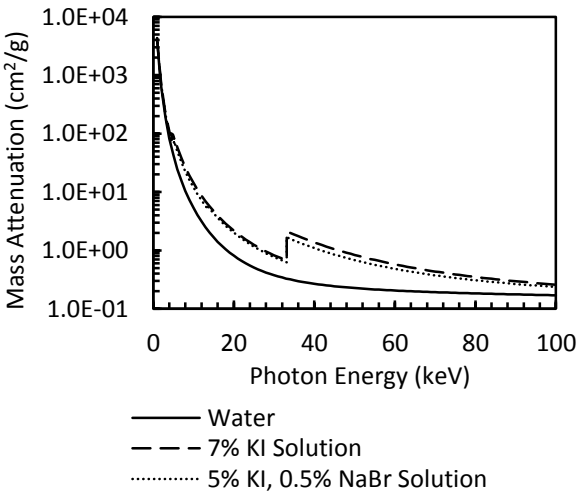

Figure 6. The X-ray mass attenuation coefficients for pure water, water with potassium iodide, and water with potassium iodide and sodium bromide.

Because of its low cost and ease of handling, potassium iodide is a common X-ray contrast material. However, when adding a contrast material, care must be taken to avoid altering the properties of the fluid so that the flow is still representative of a real spray [11].

Figure 6 shows the X-ray mass attenuation coefficients for pure water, water with 7.0% by mass potassium iodide, and water with 5.0% by mass potassium iodide and 0.5% by mass sodium bromide, generated using the XCOM database [14]. The attenuation for both contrast agent mixtures are higher across the entire spectrum than for pure water. However, the biggest improvement is at 33 keV where the K-edge for iodine occurs. Unfortunately, 33 keV is above much of the flux for the white beam spectrum, particularly with the unfiltered beam. The K-edge for bromine is more useful, occurring at 13.5 keV, which is near the peak flux of the unfiltered white beam. Unfortunately, the concentration of sodium bromide was too low in this experiment for it to make a significant impact. Finally, it should be noted that, while the contrast agents improve attenuation at the higher photon energies, the attenuations at these energies are still an order of

magnitude or more lower than the attenuations at 10 keV and below, indicating that optimizing the beam spectrum should be the first course of action to improve imaging, and contrast agents used only if beam spectrum optimization proves insufficient.

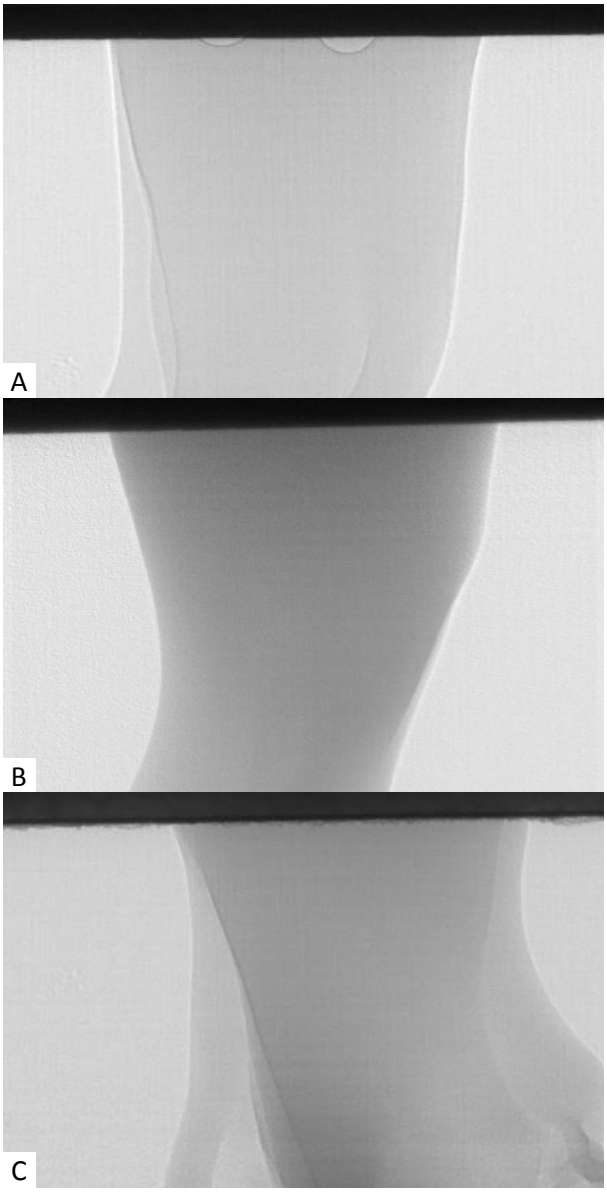

Figure 7. The effect of adding contrast material to the liquid of a spray. The liquids are A) water, B) water with 7.0% potassium iodide, and C) water with 5.0% potassium iodide and 0.5% sodium bromide.

To demonstrate the effects of contrast agents on the imaging of a real spray, the three fluids were each imaged with the unfiltered white beam. The results of this are shown in Figure 7. It is clear that the liquid with contrast material added has more contrast with the background than does water only. This is consistent with what the mass attenuation coefficients predict. However, from the images alone, there is no clear difference between the 7 % KI solution and the 5% KI and 0.5% NaBr solution. To demonstrate the differences more clearly, the row of pixels 100 μm downstream of the nozzle exit is plotted for each image (Figure 8). From this data, it is clear that, as predicted, the KI and NaBr solution is slightly less attenuating than the KI only solution. However, this is largely a function of the amount of contrast material used.

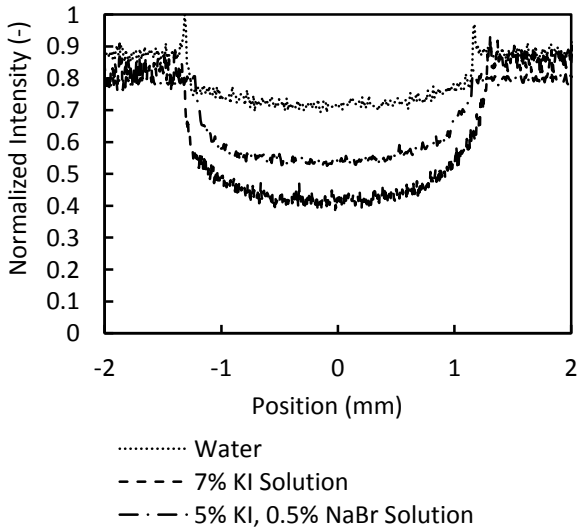

Figure 8. The normalized intensity of the spray radiographs, with different contrast agents added, at 100 μm downstream of the nozzle exit.

One final note on adding contrast material – in addition to the possibility of the contrast material changing the properties of the fluid, it is also possible for the contrast agent to come out of solution and form deposits. During the experiments with the KI contrast material, after many hours of operating the spray, a large deposit of KI formed on the inside of the gas nozzle, adhering to the outside wall of the liquid needle (shown in Figure 9). Therefore, it is strongly recommended that any experiments using contrast material be checked regularly for deposits of contrast material and then remove the deposits if necessary.

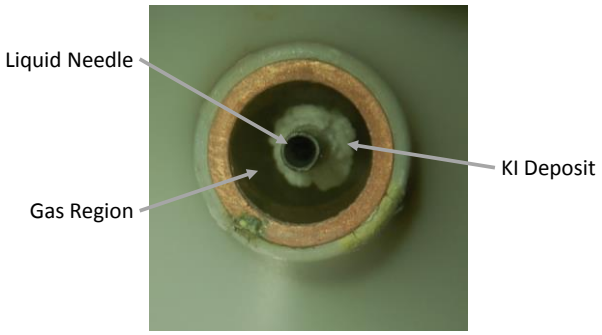

Figure 9. A deposit of KI contrast material that formed inside the spray nozzle after many hours of operation.

Effect of Scintillators

The choice of scintillator changes the X-ray image in two primary ways. First, the choice of scintillator material effects how efficient X-ray photons are converted into visible light for imaging and how long it takes for the emitted visible light to decay. Both the YAG and LuAG scintillator used in this study are high efficiency, fast decay materials. The second, and in this study more important, parameter is the thickness of the material. A thicker scintillator is able to capture more X-ray energy and thus generate more visible light. However, at the high magnifications at which the imaging system is operating at, the depth of field of the optics is very small, so having a thicker scintillator can also cause image blurring if it is thicker than the depth of field of the imaging optics. To test this, an Xradia X-ray resolution test pattern was imaged with both the 500 μm thick YAG scintillator and the 100 μm thick LuAG scintillator. As shown in Figure 10, the YAG scintillator generates more light; however, it is also significantly lower contrast than the LuAG. No filters were used on the X-ray beam for testing the scintillator materials.

Conclusions

The results of testing various white beam X-ray imaging parameters have shown that selecting the right parameters can have a significant effect on the quality of data. Since sprays are a relatively thin medium, typically using a minimally X-ray attenuating liquid, it has been shown that the use of filters on the white beam can be counterproductive. While they reduce beam hardening effects in systems with thicker, more attenuating media, in sprays, filters reduce the available flux and shift the X-ray spectrum to a higher energy, where the liquid is much less attenuating. Adding a contrast agent has been shown to be an effective way to improve spray imaging; however, users are cautioned to be careful with the contrast agent used to minimize unintended effects on the spray such as changes to fluid properties or deposition of contrast material on the spray nozzle. Finally, while thicker scintillators provide more light for imaging, they also blur the image when used in conjunction with high magnification optics. With these items in mind, it is recommended that users optimize their white beam X-ray imaging of sprays by first maximizing the low energy portion of the white beam spectrum by using as little filtering as possible, then use as thin a scintillator as possible while still providing sufficient light for imaging, and finally use contrast agents to improve image contrast only if it cannot be avoided.

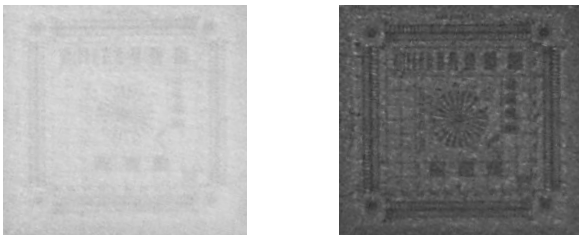

Figure 10. Xradia test pattern image with the white beam at 7-BM using a 500 um thick YAG scintillator (left) and 100 um thick LuAG scintillator (right).

Acknowledgments

This work was sponsored by the Office of Naval Research (ONR) as part of the Multidisciplinary University Research Initiatives (MURI) Program, under grant number N000141612617. The camera was purchased through an ONR Defense University Research Instrumentation Program (DURIP) grant number N000141812380. The views and conclusions contained herein are those of the authors only and should not be interpreted as representing those of ONR, the U.S. Navy or the U.S. Government.

This work was performed at the 7-BM beamline of the Advanced Photon Source, a U.S. Department of Energy (DOE) Office of Science User Facility operated for the DOE Office of Science by Argonne National Laboratory under Contract No. DE-AC02-06CH11357.

References

1. Heindel T.J., *Journal of Fluids Engineering* 133(7):074001 (2011).
2. Franka N.P., Heindel T.J., *Powder Technology* 193(1):69–78 (2009).
3. Halls B.R., Gord J.R., Schultz L.E., Slowman W.C., Lightfoot M.D.A., Roy S., Meyer T.R., *International Journal of Multiphase Flow* 109:123–130 (2018).
4. Heindel T.J., *Atomization and Sprays* 28(11):1029–1059 (2018).
5. MacPhee A.G., Tate M.W., Powell C.F., Yue Y., Renzi M.J., Ercan A., Narayanan S., Fontes E., Walther J., Schaller J., Gruner S.M., Wang J., *Science* 295(5558):1261–1263 (2002).

6. Kastengren A., Powell C.F., Arms D., Dufresne E.M., Gibson H., Wang J., *Journal of Synchrotron Radiation* 19(4):654–657 (2012).
7. Morgan T.B., Bothell J.K., Li D., Heindel T.J., Aliseda A., Machicoane N., Kastengren A.L., *Proceedings of the 14th Triennial International Conference on Liquid Atomizatin and Spray Systems (ICLASS 2018)*, Chicago, IL, USA, July 2018.
8. Kastengren A., Powell C.F., *Experiments in Fluids* 55(3):1686 (2014).
9. Bothell J.K., Li D., Morgan T.B., Heindel T.J., Aliseda A., Machicoane N., Kastengren A.L., *Proceedings of the 14th Triennial International Conference on Liquid Atomizatin and Spray Systems (ICLASS 2018)*, Chicago, IL, USA, July 2018.
10. Ketcham R.A., Carlson W.D., *Computers & Geosciences* 27(4):381–400 (2001).
11. Halls B.R., Morgan T.B., Heindel T.J., Meyer T.R., Kastengren A.L., *52nd Aerospace Sciences Meeting*, National Harbor, MD, USA, 2014, pp. AIAA 2014-0736.
12. Machicoane N., Aliseda A., *Proceedings of ILASS-Americas 29th Annual Conference of Liquid Atomization and Spray Systems*, Atlanta, GA, USA, May 2017.
13. Sánchez del Río M., Dejus R.J., *Proceedings Volume 8141, Advances in Computational Methods for X-ray Optics II*, San Diego, California, USA, September 2011, pp. 814115.
14. Berger M.J., Hubbell J.H., Seltzer S.M., Chang J., Coursey J.S., Sukumar R., Zucker D.S., Olsen K., "XCOM: Photon Cross Section Database," NIST, NBSIR 87-3597, 2010.
15. Van Nieuwenhove V., De Beenhouwer J., De Carlo F., Mancini L., Marone F., Sijbers J., *Optics Express* 23(21):27975–27989 (2015).